Analysis of diabetes mellitus screening method based on electrical properties of cells using dielectric method

Muhammad Faisal[1], *Unggul Pundjung* Juswono[1*], *Didik Rahadi* Santoso[1], and *Chomsin Sulistya* Widodo[1]

[1]Department of Physic, Brawijaya University, Jawa Timur 65145, Indonesia

Abstract. Diabetes mellitus is one of the most dangerous diseases in the world because every year, people with diabetes always increase. Methods development for diagnosing diabetes mellitus was carried out to obtain better results. This study aims to analyze diabetes mellitus screening methods based on the electrical properties of cells using the dielectric method. This study used 90 mice (*Mus musculus*) as experimental subjects. Mice were divided into six groups: one group without streptozotocin injection (Control) and five groups injected with streptozotocin. Streptozotocin doses given were 10 mg/KgBW (P1), 15 mg/KgBW (P2), 20 mg/KgBW (P3), 25 mg/KgBW (P4), and 30 mg/KgBW (P5). Mice that had experienced hyperglycemia had their dielectric constant measured using electrical impedance spectroscopy (EIS), and changes in cell morphology were observed using a binocular microscope. The results showed that the dielectric constant value of the control group was 35000, the pre-diabetes group (P1 and P2) was 35000 to 20000, while the acute diabetes mellitus group (P3, P4, and P5) was below 20000. The results of histopathological observations identified five types of specific cell damage, namely microcytes (9%), hypochromic (11%), burr cells (20%), schistocytes (20%), and macrocytic hypochromic (40%). Electrical properties of cells in the form of dielectric constants can show area dispersion at different levels of diabetes. The results of dielectric constant measurements correlate with the histopathological picture. Percentage of accumulated damage is 32% (P1); 40% (P2); 55% (P3); 65% (P4); and 74% (P5). The dielectric method can be used as an alternative method for screening diabetes mellitus based on the electrical properties of cells.

1 Introduction

Diabetes mellitus is a chronic metabolic disease characterized by elevated blood sugar levels due to insulin deficiency, insulin resistance, or a combination of both. As one of the leading causes of morbidity and mortality worldwide, early detection of diabetes mellitus is critically important in reducing the number of affected individuals. According to the International Diabetes Federation (IDF), there are 537 million people in the world suffering from diabetes

* Corresponding author: unggul-pj@ub.ac.id

mellitus in 2021. This figure is predicted to rise to 643 million people in 2030 [1][2]. Several methods for diagnosing diabetes mellitus that are commonly used are random blood sugar test (RBST), fasting blood sugar test (FBST), and oral blood sugar tolerance test (OBST) [3][4]. These three methods have weaknesses in the form of examination results that cannot be seen in real-time, are influenced by the researcher's experience, and have specific protocols that patients must follow [5].

Methods for diagnosing diabetes mellitus continue to be developed to obtain more accurate results in a shorter time. Several methods for diagnosing diabetes are currently being developed, including measuring insulin sensitivity, identifying metabolic results of people with diabetes, and examining certain micrsobes and bacteria in the digestive tract of diabetes patients [6, 7, 8]. Some of these alternative methods have higher accuracy than previous studies, but the price is still relatively expensive and not available in general health facilities [9]. Given the issues, this study aimed to examine a diabetes mellitus screening approach that is easier, faster, cheaper, and more accurate by utilizing the dielectric properties of materials.

A dielectric method is one method of observing the electrical properties of cells that are often used in medical tomography [10]. Diagnosis based on the electrical properties of cells works by identifying changes, damage, or abnormalities in a cell. Each different disease has a different cell electrical pattern [11]. Cells in living bodies are bound by cell membranes, which can regulate the balance between intracellular and extracellular charges in cells [12]. Charges distributed in the cell will be arranged randomly when there is no influence of an external electric field and will become orderly when influenced by an external electric field. This interaction between charges can occur in molecules with good dipole moments [13].

Dipole moment in biological materials is influenced by temperature, degree of acidity, and material's ability to polarize when charges are distributed [14][15]. Diabetes blood cells are a dielectric material that is polar because they have freely distributed charges. Diabetes blood cells are polar molecules with a dipole moment that is not equal to zero [16]. The research aim was to analyze the electrical properties of mice (*Mus musculus*) blood cells in classifying levels of diabetes mellitus based on dielectric properties. Histopathological observations of blood cells will also be carried out to see specific damage types that occur during diabetes mellitus. This study focuses on developing a simpler method for diagnosing diabetes mellitus using dielectric techniques. The dielectric method offers more advantages than conventional methods, thereby enhancing the accessibility of diagnosis, especially in areas with limited medical resources. This research is expected to provide a new, more effective alternative for diabetes mellitus screening, broaden insights into diabetes diagnosis, and promote further development of innovative technologies in the healthcare field.

2 Materials and methods

2.1 Preparation of experimental animals

This study used 90 male mice (*Mus musculus*) of the BALB/c strain, weighing 29 ± 1 grams and aged 3 months. All mice were standard laboratory mice obtained from Brawijaya University. Diabetes mellitus induction in the mice was carried out by injecting streptozotocin (dissolved in 0.1 M citrate buffer, pH 4.5) for seven consecutive days. Streptozotocin was administered via intraperitoneal (IP) injection once daily. The mice received a 10% dextrose solution after streptozotocin injection to prevent sudden hypoglycemia. Before the streptozotocin injections, the mice were acclimatized for seven days in a controlled cage environment maintained at a stable temperature of 25 ± 2°C, humidity of 46 ± 7%, and a 12-hour light/dark cycle in the Biophysics Laboratory. Following the acclimatization phase, the mice were divided into six groups: one without streptozotocin

injection (Control) and five receiving streptozotocin injections. The streptozotocin doses administered were 10 mg/kgBW (P1), 15 mg/kgBW (P2), 20 mg/kgBW (P3), 25 mg/kgBW (P4), and 30 mg/kgBW (P5). The control group mice did not receive streptozotocin injections and were fed the same diet as the other groups, which consisted of starch- and cellulose-based food [17].

2.2 Measurement of electrical properties based on dielectric method

The measurement of the dielectric properties of blood tissue was conducted using the dielectric method. Blood tissue from each group was collected through the tail vein. Blood was collected by dipping the mice's tail into warm water (at approximately 40 °C for 30-40 seconds) to dilate the blood vessels. Afterwards, the mice's tail was dried using tissue and sterilized with alcohol to prevent infection. Blood was drawn through the tail vein using a small needle (such as an insulin needle) and then placed into an acrylic chamber, with both sides clamped using parallel plate electrodes (Figure 1). The parallel plate electrodes were connected to the Electrical Impedance Spectroscopy using a bayonet nut connector (BNC). Electrical impedance spectroscopy is an instrument that provides current injection and reads the output signal from the measurement. The frequency installed on a tool is 100 Hz to 100 KHz.

$$\varepsilon_r = \frac{C.d}{\varepsilon_0.A} \quad (1)$$

The results of measuring electrical properties will be displayed on a PC monitor screen in the form of a capacitance value (C), which can be used to calculate the dielectric constant (ε_r) through equation 1. The cross-sectional area of plate (A) and distance between parallel plates (d) is measured previously, and then values of air permittivity (ε_0 = 8.85x10^{-12} F / m) refers to the reference.

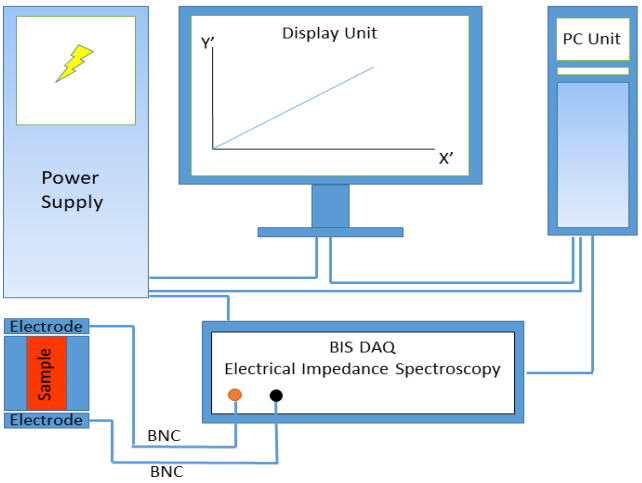

Fig 1. Illustration of measurements using the dielectric method.

2.3 Histopathological observation

Histopathological observations were carried out to see the type of cell damage in each treatment group. Method for staining and making preparations was carried out as was the previous observation procedure [18]. We analyzed the number of cells experiencing

hypocromia, macrocyte hypocromia, schistocytes, microcytes, and burr cells. The percentage of cell damage is calculated through the equation 2.

$$\text{Percentage of cell damage} = \frac{\Sigma \text{ damage cells}}{\Sigma \text{ observed cells}} \times 100\% \quad (2)$$

2.4 Blood sugar measurement

Blood sugar levels were measured as a standard test, and the data were compared to identify diabetes mellitus. The fasting blood sugar test (FBS) was the blood sugar level test method. Mice were fasted for 12 hours before their blood sugar levels were measured using a calibrated glucometer with an accuracy of ≥ 90%, as stated in the device specifications [19].

2.5 Statistical analysis

Analysis of Variance (ANOVA) and Pearson correlation were used to evaluate statistical significance and differences between groups. Calculations were performed using the Statistics 13.0 software [10]. ANOVA tests with a p-value < 0.05 were considered statistically significant. A correlation coefficient value of r = 1 indicates a perfect positive relationship, r = -1 indicates a perfect negative relationship and r = 0 indicates no linear relationship between the two variables.

3 Results and discussions

Streptozotocin injection treatment has caused mice to develop diabetes mellitus with different blood sugar levels in each group (Figure 2). The control group had blood sugar levels below 100 mg/dL. Groups P1 and P2 had blood sugar levels between 150 mg/dL to 200 mg/dL, which indicated that the mice had pre-diabetes mellitus. Groups P3, P4, and P5 had blood sugar levels above 300 mg/dL, which indicated that the mice had acute diabetes mellitus. Blood sugar levels rise due to low insulin production in the body. Low insulin production is caused by damage to pancreatic beta cells due to the influence of streptozotocin [20][21].

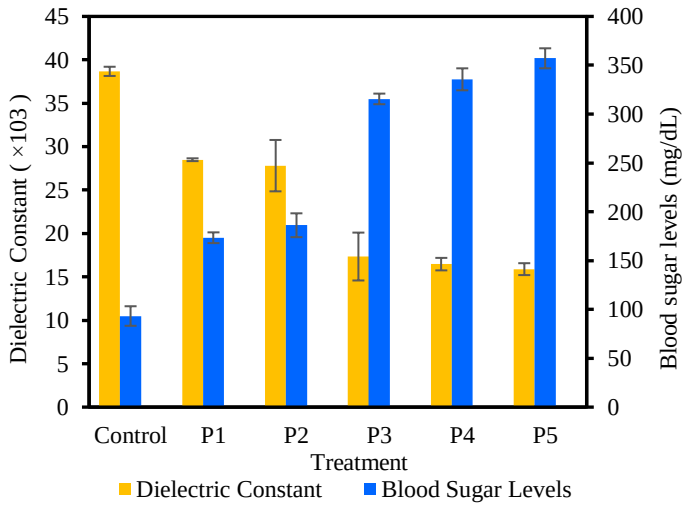

Fig 2. Correlation of streptozotocin treatment with blood glucose levels and dielectric constant.

The results of the dielectric constant measurements are also shown in Figure 2. The control group has a dielectric constant value above 35000, groups P1 and P2 have dielectric constants between 35000 and 20000, and groups P3, P4, and P5 have dielectric constant values below 20000. Dielectric constant value correlates with the results of measuring blood sugar levels. The relationship between dielectric constant and blood sugar levels is consistently inversely proportional. When blood sugar levels rise, the dielectric constant value decreases. This incident proves that dielectric properties can be used as a reference for screening diabetes mellitus in the body. Mice that have pre-diabetes mellitus have different dielectric constant values from mice that have diabetes mellitus. The dispersion graph of the dielectric constant shows that high sugar levels will form different physicochemical properties of materials from low blood sugar levels. Electric dipole moment, chemical compound composition, water content, temperature, viscosity, material structure, and degree of acidity are variables that greatly influence the dielectric characteristics of materials [22].

Dielectric constant values decrease that occurred in each group was 26% (P1), 28% (P2), 55% (P3), 57% (P4), and 59% (P5). A decrease in the dielectric constant with the same diabetes category shows a range of differences that is not too far away. In contrast, a decrease in dielectric constant with a different diabetes category will show a very large range of differences. This event was demonstrated by mice that both experienced pre-diabetes mellitus in groups P1 and P2. Two only have a dielectric constant difference of 2%. The same event occurred in acute diabetes mellitus mice in groups P3, P4, and P5. The difference in dielectric constant is only 2%. When compared between dielectric constants of pre-diabetes and diabetes mellitus groups, the difference is very large (± 20%). This phenomenon is interesting because there is a consistent pattern between dielectric properties and the classification of diabetes mellitus that occurs in mice.

Based on statistical analysis, blood sugar levels, and dielectric constant values yielded a p-value of 7.8×10^{-5} with a correlation coefficient $r = -0.98$. These results indicate a statistically significant difference between blood sugar levels and dielectric constant values. Furthermore, the findings demonstrate that the variation between blood sugar levels and dielectric constant values under different treatments is not due to random chance but represents a meaningful difference. The very small p-value (< 0.05) suggests that these results are highly statistically significant, making it highly likely that the negative relationship is true and not coincidental. The correlation coefficient $r = -0.98$ indicates a very strong negative relationship between blood sugar levels and dielectric constant values. This negative correlation implies that the dielectric constant value decreases almost perfectly as blood glucose levels increase.

Histopathological observations showed blood cell deformation in each treatment group, as shown in Figure 3. The control group had blood cells that were still round with cell wall lines that were still clearly visible, and no degradation or changes in cell morphology were found. The pre-diabetes mellitus group (P1 and P2) showed irregular changes in cell wall lines, so uneven degradation was seen at each boundary between cells. The diabetes mellitus group (P3, P4, and P5) showed changes in cell wall lines evenly distributed throughout the observation field. Boundaries between one cell and another become invisible. Even for group P5, the cell walls look weathered like melting ice. This event shows that the cell walls of the diabetes mellitus group have lost the stability of the cytoskeleton and integrity of the cell membrane. Many cell injuries and inflammation cause the number of normal cells to decrease.

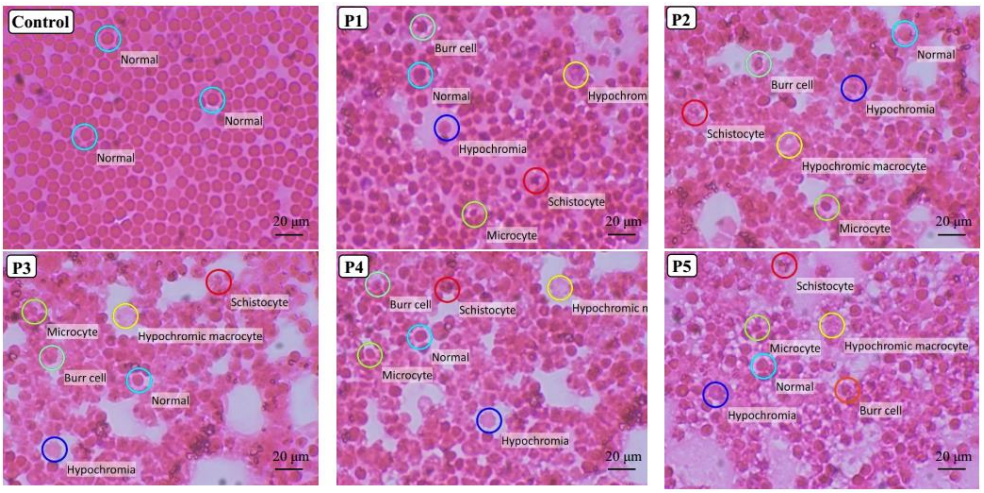

Fig 3. Histopathological observation of blood cells. The group without streptozotocin injection **(Control)**, the group injected with streptozotocin at a dose of 10 mg/KgBW **(P1)**, a dose of 15 mg/KgBW **(P2)**, a dose of 20 mg/KgBW **(P3)**, a dose of 25 mg/KgBW **(P4)**, and a dose of 30 mg/KgBW **(P5)**.

Five types of specific cell damage were identified namely hypochromic, macrocyte hypochromic, schistocyte, microcyte, and burr cell. Red blood cells that experience hypochromia are found in cells with a faded colour due to low haemoglobin concentration and iron deficiency. Low haemoglobin concentration makes the body more susceptible to fatigue and weakness [23]. Macrocyte hypocromia is different from ordinary hypocromia because the size of red blood cells is larger than that of other normal blood cells. The condition of macrocyte hypochromia also causes red blood cells to become duller in colour and degraded so that the edges of cells look like melting ice [24]. Microcyte damage shows that red blood cells are smaller than their normal size. Microcytes make red blood cells more intensely coloured. Microcytes can occur due to chronic inflammation, which disrupts iron metabolism and causes microcytic anaemia. Burr cell (echinocyte) condition is indicated by the presence of red blood cells that are shaped like spiked balls due to loss of cytoskeleton stability and cell membrane integrity [25]. This event will produce further impacts in the form of a schistocyte condition or a change in the shape of red blood cells that are fragmented and irregular [26].

The percentage graph of red blood cell damage consistently increases for each type of damage (Figure 4). Microcytes were the least common cell damage found, while macrocyte hypochromia was the most common. Cell damages number that occurred respectively were microcytes (9%), hypochromic (11%), burr cells (20%), schistocytes (20%), and macrocyte hypochromic (40%). Histopathological observations show that diabetes mellitus is most susceptible to causing a decrease in haemoglobin concentration and iron deficiency, so that type of macrocyte hypochromia damage is most often found in the blood.

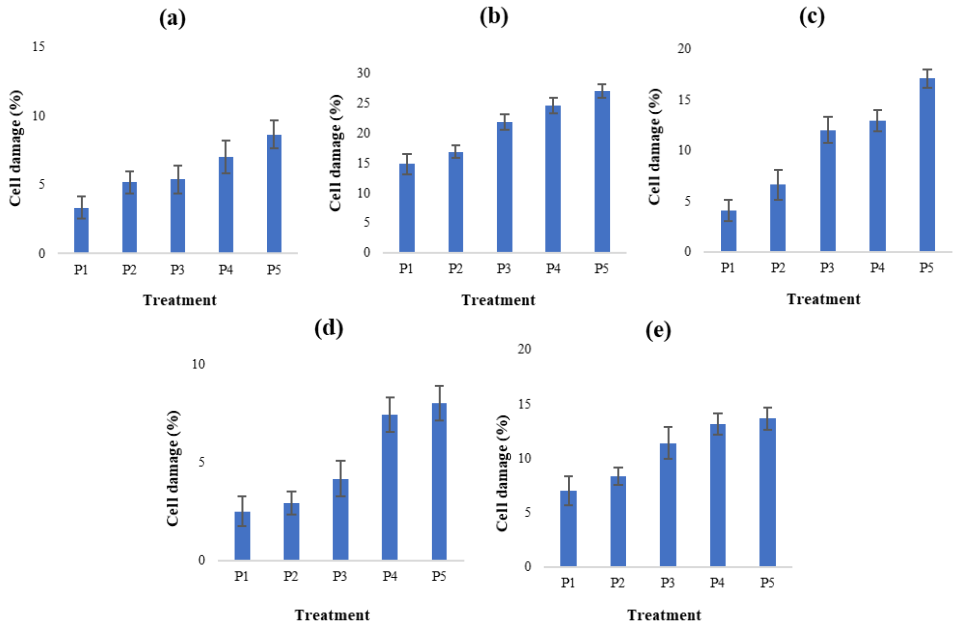

Fig 4. Percentage of each type of cell damage. **(a)** hypochromia, **(b)** macrocyte hypochromia, **(c)** schistocytes, **(d)** microcytes, and **(e)** burr cells.

The relationship between one type of cell damage and other cell damage cannot be separated from each other because they are interconnected. Diabetes mellitus forces cells to undergo deformation due to chronic and complex metabolic disorders in the body. Based on a statistical analysis of five types of blood cell damage (hypochromia, macrocyte hypochromia, microcyte, burr cell, and schistocyte) obtained, a p-value of 1.4×10^{-5}. This result shows a statistically significant difference for each type of cell damage. This result also explains that the increase in the percentage of cell damage does not occur by chance but has a significant difference. A very small p-value indicates that this result is statistically significant, so this positive relationship is likely to be true and not just a coincidence. The Pearson correlation analysis obtained a very strong relationship with a value of $r = 0.91$ to $r = 0.99$. This result shows an almost perfect positive relationship between the five types of blood cell damage (hypochromia, macrocyte hypochromia, microcyte, burr cell, and schistocyte).

Based on the results of the Pearson correlation analysis, it is known that the highest correlation coefficient value occurs in macrocyte hypochromia with burr cells which has a correlation coefficient of $r = 0.99$ (almost approaching a perfect positive relationship). The lowest correlation coefficient value occurs in microcyte damage with schistocytes, with a correlation coefficient of $r = 0.91$ (still indicating a strong positive relationship). A strong positive relationship indicates that an increase in one type of cell damage tends to affect other types of cell damage through physiological or pathological mechanisms.

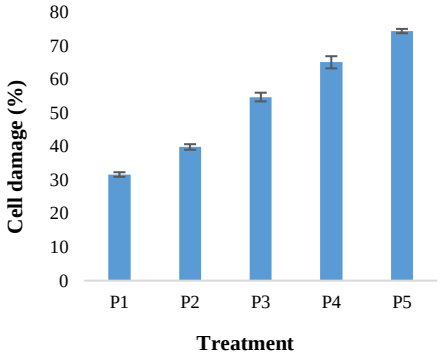

Fig 5. Percentage of accumulated cell damage.

Cell damage that appears is caused by previous cell damage. This condition will occur in a chain that causes complications in tissue and organ systems [27]. The percentage of accumulated cell damage is shown in Figure 5. Accumulated damage describes all types of damage that correlate with dielectric constant measurement results.

Each treatment group's dielectric constant dispersion pattern indicates the cell's ability to store electrical energy [28]. The measured dielectric constant of blood cells shows a comparison between the permittivity of the sample and vacuum permittivity [29][30]. This event will describe the extent to which measured blood cells can inhibit and store electrical charge that passes through them [31]. Blood cells are a dielectric material with weak electrical conductivity and can store electrical charges like a capacitor [32]. This phenomenon can occur because the blood cell membrane has a double-layered lipid structure like a capacitor, where the membrane head is polar, and the membrane tail is non-polar. Normal cell membranes can retain charged ions outside the cell from entering the cell [33]. The cell membrane is important in regulating conditions inside and outside the cell. Every substance that enters and exits the cell will be selected and then adjusted to the amount needed by the cell membrane [34, 35].

A healthy cell membrane can block substances not needed from entering the cell, but a damaged cell membrane allows substances not needed to enter and leave the cell [36] freely. High blood sugar levels will create a hyperglycemic environment around cells and can disrupt membrane integrity [37]. Normal blood cells placed in an electric field will not be easily penetrated by electric current passing through them because blood is a material that does not have free electrons moving in it [38]. This intrinsic character differentiates healthy blood tissue, like a capacitor, and damaged blood tissue, like a conductor [39]. Conductor materials can easily flow electric current with high electron mobility [40]. High mobility of electrons is caused by conductor material having charged particles that move freely in it (Figure 6) [41].

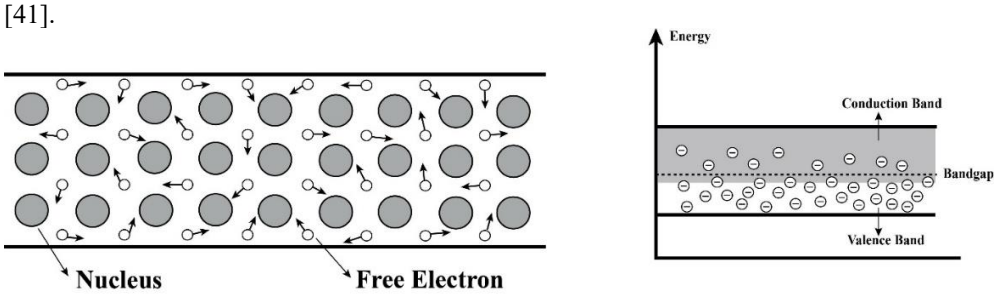

Fig 6. Illustration of charge distribution in conductor materials.

Positive and negative charges in blood cells experience movement in different directions. Positive charges will be in the same direction as the external electric field, while negative charges will be in the opposite direction to the external electric field (Figure 7) [42, 43].

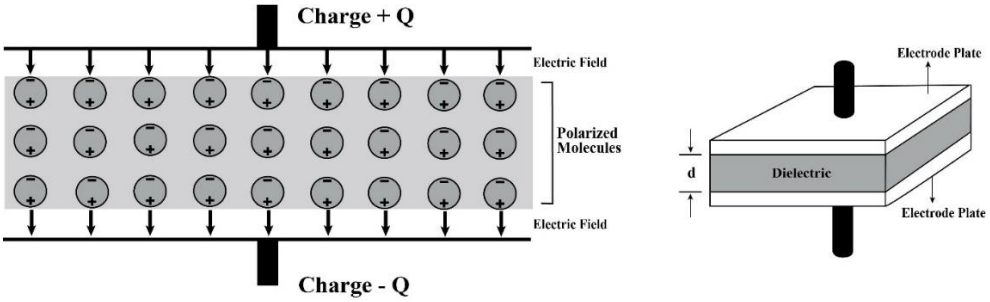

Fig 7. Illustration of charge direction in dielectric material.

The charge separation phenomenon in blood tissue will cause charge polarization, reducing the electric field in dielectric material [44]. Blood samples placed between parallel plate electrodes increase the capacitance properties of the capacitor by storing opposite charges between electrode surfaces [45]. This explains why, in healthy blood tissue, charges can be perfectly polarized and have a high dielectric constant value. In contrast, blood damaged by diabetes mellitus has a low dielectric constant value (Figure 8) [46, 47].

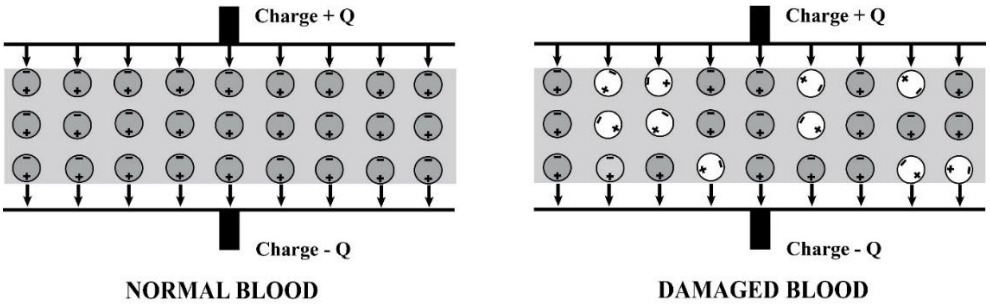

Fig 8. Differences in polarization ability of normal blood and damaged blood.

In hyperglycemia conditions, the body's metabolism is abnormal because sugar molecules in the blood are too high and cannot be converted into energy [48]. This event disrupts the citric acid cycle. A citric acid cycle is an important part of the cellular respiration process, responsible for adequate energy production in the form of ATP [49]. Disturbances in the citric acid cycle make it difficult for tissue cells to obtain ATP, which decreases phospholipid synthesis and ion pump activity [50]. Decreased phospholipid synthesis and ion pump activity will affect the stability and integrity of cell membranes [51]. Disruption of the cell membrane will disturb the balance of the electrochemical gradient, cause inflammation to emerge, damage cell structure, and cause changes in blood cell morphology. When the cell structure is damaged, its dielectric properties change [32, 52]. When dielectric material's ability to store charge changes, it will create conditions where dielectric material can begin to conduct electric current [53]. Measuring blood sugar results with pre-diabetes shows that damage is not very significant and has the potential to return to a normal state. Still, a group of mice with diabetes mellitus shows significant damage where blood cells become like conductors capable of transmitting electricity easily [54, 55]. Diabetes mellitus condition shows electric dipole moment characteristics and polarity degree of blood cells. The blood of people with diabetes mellitus has a very low ability to distribute neatly when exposed to

an external electric field. The dielectric constant low value also reflects the high water content of blood cells when they are in a hyperglycemic environment [56, 57].

4 Conclusions

Electrical properties of cells in the form of dielectric constants can show area dispersion at different levels of diabetes. Normal blood cells have a dielectric constant value above 35000, pre-diabetes mellitus blood cells have a dielectric constant between 35000 and 20000, while diabetes mellitus blood has a dielectric constant value below 20000. The results of dielectric constant measurements correlate with the histopathological picture. Percentage of accumulated damage is 32% (P1); 40% (P2); 55% (P3); 65% (P4); and 74% (P5). Blood sugar levels and dielectric constant yielded a p-value of 7.8×10^{-5} with a correlation coefficient r = -0.98. These results indicate a statistically significant difference between blood sugar levels and dielectric constant values. The dielectric method can be used as an alternative method for screening diabetes mellitus based on the electrical properties of cells.

Ethics

Ethics Committee Approval: Brawijaya University Local Ethics Committee of the host approved the research (ethics approval number: 128–KEP–UB 2023 date: 21.08.2023).

All authors declared that this research was funded by Brawijaya University Malang. Republic of Indonesia. under contract number (4160.11/UN10.F09/PN/2023).

References

1. S. Kolo, C. Mamadou, K. Raogo, A. Olivier, B. Daniel, Impact of data preprocessing and balancing on diabetes prediction using the decision tree technique. Int. J. Numer. Methods Appl. **23**, 157–80 (2023).
2. N. Aulia, E. Ernawati, Management of type 2 diabetes mellitus cases with diabetic neuropathy complication and hypertension grade ii through the approach of family medicine. Sci. Midwifery. **10**, 3869–75 (2022).
3. M. Mirzaei, M. Moosavi, E. Mansouri, S. Mohtadi, M.J. Khodayar, Diosmin exerts hepatoprotective and antihyperglycemic effects against sodium arsenite-induced toxicity through the modulation of oxidative stress and inflammation in mice J. Trace Elem. Med. Biol. **78**, 127154 (2023).
4. J. Webber, S. Mostafa, R.P. Raghavan, R.A. Round, S.E. Manley, A. Karwath, G.V. Gkoutos, G.A. Roberts, Diagnosing gestational diabetes during the Covid-19 pandemic using HbA1c rather than oral glucose tolerance test (OGTT). Diabet. Med. **102**, (2023).
5. D.G.B Krisnamurti, M. Louisa, E.H. Poerwaningsih, T.J.E. Tarigan, V. Soetikno, H. Wibowo, C.M.H. Nugroho, Vitamin D supplementation alleviates insulin resistance in prediabetic rats by modifying IRS-1 and PPARγ/NF-κB expressions. Front. Endocrinol. (Lausanne). **14**, 1089298 (2023).
6. P.B. Renz, F.C. Chume, J.R.T. Timm, A.L. Pimentel, J.L. Camargo, Diagnostic accuracy of glycated hemoglobin for gestational diabetes mellitus: a systematic review and meta-analysis Clin. Chem. Lab. Med. **57**, 1435–49 (2019).
7. P.M. Dualib, J. Ogassavara, R. Mattar, E.M.K. da Silva, S.A. Dib, B. de Almeida Pititto, Gut microbiota and gestational Diabetes Mellitus: A systematic review Diabetes Res. Clin. Pract. **180**, 109078 (2021).

8. Y. Koike, S-I. Shirabe, H. Maeda, A. Yoshimoto, K. Arai, A. Kumakura, K. Hirao, Y. Terauchi, Effect of canagliflozin on the overall clinical state including insulin resistance in Japanese patients with type 2 diabetes mellitus. Diabetes Res. Clin. Pract. **149**, 140–6 (2019).
9. S.Y. Park, J-F. Gautier, S. Chon, Assessment of insulin secretion and insulin resistance in human. Diabetes Metab. J. **45**, 641–54 (2021).
10. K. Ishfaq, M.A. Maqsood, M.A. Mahmood, S. Anwar, A.Y. Alfaify, N. Ahmad, Powder mixed electrical discharge texturing of AISI 316 for biomedical applications: an in-depth comparative study of various dielectrics and electrode materials. J. Brazilian Soc. Mech. Sci. Eng. **45**, 524 (2023).
11. Y. Wu, Y. Yue, H. Zhang, X. Ma, K. Li, W. Zeng, S. Wang, Y. Meng, Label free and high-throughput discrimination of cells at a bipolar electrode array using the AC electrodynamics. Anal. Chim. Acta. **127**, 341701 (2023).
12. J-H. Park, S. Kwon, Y.M. Park, Extracellular vimentin alters energy metabolism and induces adipocyte hypertrophy. Diabetes Metab. J. **48**, 2 (2024).
13. X. He, H. Jiang, J. Li, Y. Ma, B. Fu, C. Hu, Dipole-moment induced phototaxis and fuel-free propulsion of ZnO/Pt Janus micromotors. Small. **17**, 2101388 (2021).
14. H. Mali, V.S. Sharma, A.S. Sharma, M. Athar, S.L. Rathod, P.S. Shrivastav, H.R. Prajapati, Aroylhydrazone appended cinnamate based calamitic liquid crystal: effect of alkoxy side chain and position of terminal pyridine core on mesomorphic properties. J. Mol. Struct. **13**, 6717 (2023).
15. Y. Zhang, Z. Ouyang, Y. Dong, J. Zhao, H. Zhang, X. Li, C. Zhang, X. Tang, X. Guo, L. Zhu, Efficient removal of tetracycline by a novel bimetallic nickel/copper-loaded biochar: The crucial roles of π-π interaction and complexation. Appl. Surf. Sci. **15**, 8372 (2023).
16. V. Mazankova, K. Kostyleva, R. Horňák, P. Sťahel, Deposition of polymeric thin films from propane-butane in atmospheric pressure discharge. PLASMA Phys. Technol. **9**, 1–5 (2022).
17. B. Zhao, F. Wu, X. Han, W. Zhou, Q. Shi, H. Wang, Protective effects of acarbose against insulitis in multiple low-dose streptozotocin-induced diabetic mice. Life Sci. **263**, 118490 (2020).
18. H. Shokrani, H. Norouzian, O. Dezfoulian, Exo-erythrocytic stages of *Haemoproteus* sp. in common buzzard (*Buteo buteo*): A histopathological and molecular study Int. J. Parasitol. Parasites Wildl. **16**, 64–9 (2021).
19. Q. Wang, X. Wu, F. Shi, Y. Liu, Comparison of antidiabetic effects of saponins and polysaccharides from *Momordica charantia* L. in STZ-induced type 2 diabetic mice Biomed. Pharmacother. **109**, 744–50 (2019).
20. V. Minasian, M. Nazari, The association between type 1 diabetes and exercise/physical activity and prolongation of the honeymoon phase in patients. Life Sci. **12**, 2114 (2023).
21. C.N. Edirneli, E. Beyazçiçek, Investigation of the effects of short, medium, long chain fatty acids on osteocalcin, leptin and insulin levels Sağlık Bilim. Değer. **13**, 451–7 (2023).
22. M. Rerak, J. Makowska, K. Osińska, T. Goryczka, A. Zawada, M. Adamczyk-Habrajska, The effect of Pr doping contents on the structural, microstructure and dielectric properties of BaBi2Nb2O9. Aurivillius Ceramics Materials (Basel). **15**, 5790 (2022)
23. N.H. Dinh, S.M. Cheanh Beaupha, L.T.A. Tran, The validity of reticulocyte hemoglobin content and percentage of hypochromic red blood cells for screening iron-deficiency

anemia among patients with end-stage renal disease: a retrospective analysis. BMC Nephrol. **21**, 1–7 (2020).

24. N. KT, K. Prasad, B.M.K. Singh, Analysis of red blood cells from peripheral blood smear images for anemia detection: a methodological review. Med. Biol. Eng. Comput. **60**, 2445–62 (2022).
25. R. Bissinger, T. Nemkov, A. D'Alessandro, M. Grau, T. Dietz, B.N. Bohnert, D. Essigke, M. Wörn, L. Schaefer, M. Xiao, Proteinuric chronic kidney disease is associated with altered red blood cell lifespan, deformability and metabolism. Kidney Int. **100**, 1227–39 (2021).
26. G. Zini, G. d'Onofrio, W.N. Erber, S. Lee, Y. Nagai, G.W. Basak, J. Lesesve, and (ICSH) I C for S in H 2021, update of the 2012 ICSH Recommendations for identification, diagnostic value, and quantitation of schistocytes: Impact and revisions Int. J. Lab. Hematol. **43**, 1264–71 (2021).
27. G. Daryabor, MR. Atashzar, D. Kabelitz, S. Meri, K. Kalantar, The effects of type 2 diabetes mellitus on organ metabolism and the immune system. Front. Immunol. **11**, 1582 (2020).
28. K.K. Gleason, Designing organic and hybrid surfaces and devices with Initiated Chemical Vapor Deposition (iCVD) Adv. Mater. **23**, 6665 (2023).
29. B. Salski, A. Pacewicz, P. Kopyt, Measurement errors and uncertainties in the complex permittivity extraction with a Fabry–Perot open resonator. IEEE Trans. Microw. Theory Tech. **71**, 11 (2023).
30. F. Wang, J. Huang, H. Zhang, Q. Shen, Dielectric, piezoelectric, and ferroelectric nanomaterials in the biomedical applications. IET Nanodielectrics. **6**, 4 (2023).
31. O. Al Otaibi, M. Shkir, I.M. Ashraf, Facile auto combustion synthesis of CuO nanoparticles and their structure-opto-dielectric and photodetection performances: An effect of different citric acid concentrations. J. Photochem. Photobiol. A Chem. **11**, 5194 (2023).
32. Y. Zhu, Terahertz technologies for biosensing and biomedical analysis Front. Bioeng. Biotechnol. **11**, (2023).
33. Y. Zhou, L. Jiang, Bioinspired nanoporous membrane for salinity gradient energy harvesting. Joule. **4**, 2244–8 (2020).
34. S. Zhou, J. Hu, S. Liu, J-X. Lin, J. Cheng, T. Mei, X. Wang, H-G. Liao, L. Huang, S-G. Sun, Biomimetic micro cell cathode for high performance lithium–sulfur batteries Nano Energy. **72**, 104680 (2020).
35. H. Jain, M.C. Garg, Fabrication of polymeric nanocomposite forward osmosis membranes for water desalination—A review. Environ. Technol. Innov. **23**, 101561 (2021).
36. P. Makvandi, M. Chen, R. Sartorius, A. Zarrabi, M. Ashrafizadeh, F.D. Moghaddam, J. Ma, V. Mattoli, F.R. Tay, Endocytosis of abiotic nanomaterials and nanobiovectors: Inhibition of membrane trafficking. Nano Today. **40**, 101279 (2021).
37. S. Sharma, P. Tripathi, J. Sharma, A. Dixit, Flavonoids modulate tight junction barrier functions in hyperglycemic human intestinal Caco-2 cells. Nutrition. **78**, 110792 (2020).
38. Z. Bai, Y. Xu, C. Lee, J. Guo, Autonomously adhesive, stretchable, and transparent solid-state polyionic triboelectric patch for wearable power source and tactile sensor Adv. Funct. Mater. **31**, 2104365 (2021).

39. J. Lopes, D. Lopes, M. Pereira-Silva, D. Peixoto, F. Veiga, M.R. Hamblin, J. Conde, C. Corbo, E.N. Zare, M. Ashrafizadeh, Macrophage cell membrane-cloaked nanoplatforms for biomedical applications. Small Methods. **6**, 2200289 (2022)
40. X. Yang, W. Liu, M. De Bastiani, T. Allen, J. Kang, H. Xu, E. Aydin, L. Xu, Q. Bi, H. Dang, Dual-function electron-conductive, hole-blocking titanium nitride contacts for efficient silicon solar cells. Joule. **3**, 1314–27 (2019).
41. X. Cheng, S. Chen, Y. Lv, H. Chen, B.M. Novac, An improved high voltage pulse generator with few nanoseconds based on the synergy of DOS and LTD topologies for supra electroporation. IEEE Trans. Ind. Electron. **70** 7855–66 (2022)
42. H. Liu, B.X. Du, M. Xiao, Y.W. Ma, Effects of electromagnetic field on partial discharge behavior in BOPP film capacitors IEEE Trans. Dielectr. Electr. Insul. **30**, 6 (2023).
43. S. Das Barman, R. Shah, S. Islam, A. Kumar, Numerical model of cloud-to-ground lightning for PyroCb thunderstorms. IEEE J. Sel. Top. Appl. Earth Obs. Remote Sens. **8** (2023).
44. H.L.L. Aye, B. Lin, Y. Ishitani, Longitudinal-optical-phonon resonant thermal emission efficiency and spectrum control of metal-GaAs surface micro-stripe structures Infrared Phys. Technol. **10**, 4924 (2023).
45. H. Tu, S. Wang, H. Jiang, Z. Liang, D. Shi, Y. Shao, J. Shen, Y. Wu, X. Hao, Enhanced performance of supercapacitors by constructing a "mini parallel-plate capacitor" in an electrode with high dielectric constant materials. J. Mater. Chem. A. **8**, 166 (2020).
46. O. Ciftja, Electrostatic interaction energy between two coaxial parallel uniformly charged disks Results Phys. **15**, 102684 (2019).
47. A.M. Najarian, M. Supur, R.L. McCreery, Electrostatic redox reactions and charge storage in molecular electronic junctions. J. Phys. Chem. C. **124**, 1739–48 (2019).
48. M. Veit, R. van Asten, A. Olie, P. Prinz, The role of dietary sugars, overweight, and obesity in type 2 diabetes mellitus: A narrative review. Eur. J. Clin. Nutr. **76**, 1497–501 (2022).
49. X. Hu, J.D. Chandler, S. Park, K. Liu, J. Fernandes, M. Orr, M.R. Smith, C. Ma, S-M. Kang, K. Uppal, Low-dose cadmium disrupts mitochondrial citric acid cycle and lipid metabolism in mouse lung. Free Radic. Biol. Med. **131**, 209–17 (2019).
50. L. Yu, W. Li, J. Chu, C. Chen, X. Li, W. Tang, B. Xia, Z. Xiong, Uranium inhibits mammalian mitochondrial cytochrome c oxidase and ATP synthase. Environ. Pollut. **271**. 116377 (2021).
51. R.J. Clarke, K.R. Hossain, K. Cao, Physiological roles of transverse lipid asymmetry of animal membranes. Biochim. Biophys. Acta (BBA)-Biomembranes. **18**, 183382 (2020).
52. Z. Yan, T. Zhang, Y. Wang, S. Xiao, J. Gao, Extracellular vesicle biopotentiated hydrogels for diabetic wound healing: The art of living nanomaterials combined with soft scaffolds. Mater. Today Bio. **10**, 810 (2023).
53. S. Karadaş, S.A. Yerişkin, M. Balbaşı, Y. Azizian-Kalandaragh, Complex dielectric, complex electric modulus, and electrical conductivity in Al/(Graphene-PVA)/p-Si (metal-polymer-semiconductor) structures. J. Phys. Chem. Solids. **148**, 109740 (2021).
54. J. Li, P. Zou, S.W. Chiang, W. Yao, Y. Wang, P. Liu, C. Liang, F. Kang, C. Yang, A conductive-dielectric gradient framework for stable lithium metal anode. Energy Storage Mater. **24**, 700–6 (2020).
55. B. Gopi, G. Ramesh, J. Logeshwaran, An innovation for energy release of nuclear fusion at short distance dielectrics in semiconductor model ICTACT. J. Microelectron. **8**, 1430 (2022).

56. M.J.M. Ridzuan, M.S.A. Majid, A. Khasri, E.M. Cheng, Z.M. Razlan, Effect of natural filler loading, multi-walled carbon nanotubes (MWCNTs), and moisture absorption on the dielectric constant of natural filled epoxy composites. Mater. Sci. Eng. B. **262**, 114744 (2020).
57. Y. Zhong, P. Wang, B. Zhang, C. Cao, X. Du, D. Duan, Y. Ni, Y. Wang, Composite dielectric model for cement concrete considering water saturation. J. Mater. Civ. Eng. **35**, 4023170 (2023).